AN INSTITIÚID UM THAIGHDE EACNAMAÍOCHTA AGUS SÓISIALTA
ESRI ECONOMIC & SOCIAL RESEARCH INSTITUTE

ESRI Working Paper No. 764

November 2023

A linear reduced-order model for the activated sludge process for the integration into a mixed-integer linear energy system optimisation model

Dana Kirchem[a,b], Matteo Giberti[c], Recep Kaan Dereli[c], Juha Kiviluoma[d], Muireann Á. Lynch[a] and Eoin Casey[b]

a: Economic and Social Research Institute, Dublin, Ireland
b: German Institute for Economic Research (DIW Berlin)
c: University College Dublin, Ireland
d: VTT Technical Research Centre of Finland Ltd

* Corresponding author:
Muireann Á. Lynch
Economic and Social Research Institute
Whitaker Square, Sir John Rogerson's Quay
Dublin 2
Email: muireann.lynch@esri.ie

Acknowledgements:
This work has emanated from research supported in part by a research grant from Science Foundation Ireland (SFI) under the SFI Strategic Partnership Programme Grant number SFI/15/SPP/E3125 and additional funding provided by the UCD Energy Institute and the Economic and Social Research Institute. The opinions, findings and conclusions or recommendations expressed in this material are those of the author(s) and do not necessarily reflect the views of the Science Foundation Ireland. Juha Kiviluoma acknowledges funding from the Academy of Finland, grant number 348093.

Abstract

Conventional wastewater treatment plants consume significant amounts of electricity. The constant aeration of the wastewater in order to foster the growth of microorganisms or the pumping of wastewater are two examples for energy-intensive processes within a plant. Case studies have shown that switching off blowers and inlet pumps for a certain period of time is possible without a loss in water quality. This yields a potential for wastewater treatment plants to provide demand response (DR) to the power system and thereby increase overall system flexibility. So far, the DR potential has only been quantified for individual plants, while the effects of large-scale DR provision by the wastewater treatment sector for the power system have not yet been studied. One reason for this is the lack of optimisation models which include both the wastewater treatment process and the power system operation in sufficient detail. Our model tackles this gap in the literature by providing a reduced-order linear biochemical model for the activated sludge process within a WWTP that can be incorporated into an operational energy system model. The results show that the effluent concentrations are predicted well by the linear reduced-order model in comparison to the results of the Standard Activated-Sludge model No. 1 (ASM1). Potential model applications are the variation of the airflow rate within a certain range and the variation of liquid influent flow rate to the system, which is a result of electricity load shedding of the inlet pumps and the blowers connected to the activated sludge tank.

Keywords: linear biochemical model; wastewater; energy system; ASM1

Nomenclature

α_1	Share of heterotrophs in the influent
α_2	Share of heterotrophs in the aerated tank
β	Share of autotrophs
η_X	Share of biomass concentration in the effluent
γ_{DO}	Correction factor for re-circulation of DO
μ_A	Autotrophic specific growth rate $[d^{-1}]$
μ_H	Heterotrophic specific growth rate $[d^{-1}]$
$\widetilde{D}$	Dilution factor $\frac{\overline{Q}}{\overline{V}}$
Air	Airflow rate $[m^3/d]$
b_A	Autotrophic decay rate $[d^{-1}]$
b_H	Heterotrophic decay rate $[d^{-1}]$
DO	Dissolved oxygen concentration $[g/m^3]$
DO_{sat}	Dissolved oxygen saturation concentration $[g/m^3]$
f_P	Fraction of biomass yielding particulate products
h	Immersion depth of diffusers [m]
i_{XB}	Nitrogen content in biomass [g N]
i_{XP}	Nitrogen content in products from biomass [g N]
k_a	Ammonification rate $[m^3$ (g COD day)$^{-1}]$
k_d	Decay rate of microorganisms $[d^{-1}]$
k_h	Max. specific hydrolysis rate [g slowly biodeg. COD (g cell COD day)^1]
K_S	Half-saturation coefficient (hsc) for heterotrophs [g COD m^3]
K_X	Hsc for hydrolysis of slowly biodegradable substrate [g slowly biodeg. COD (g cell COD day)^1]

K_{NH} Ammonia hsc for autotrophs [g NH^3Nm^3]

K_{OA} Oxygen hsc for autotrophs [g O^2 m^3]

K_{OH} Oxygen hsc for heterotrophs [g O^2 m^3]

$n \in N$ Node in Backbone

$nns \in NNS$ Node pairs of nodes which have a state connection (e.g. diffusion) in Backbone

OU_{20} Oxygen utilization rate $[g/(m^3 \cdot m)]$

p_n^{decay} Decay parameter of biomass in Backbone

p_n^{decay} Recycling parameter of biomass in Backbone

$p_{n',n}^{diffusionIn}$ Incoming diffusion parameter in Backbone

$p_{n',n}^{diffusionOut}$ Outgoing diffusion parameter in Backbone

$p_u^{efficiency}$ Efficiency parameter of a unit in Backbone

$p_n^{selfdischarge}$ Self discharge parameter in Backbone

$p_q^{thresholdLow}$ Lower influent threshold of WWTP model in Backbone

$p_q^{thresholdUp}$ Upper influent threshold of WWTP model in Backbone

$p_{n,n'}^{transferLoss}$ Transfer loss parameter in Backbone

Q_t Liquid wastewater flow $[m^3/d]$

Q_{in} Influent flow $[m^3/d]$

$q_{q,t} \in Q$ Binary variable for the influent category

S Substrate $[g/m^3]$

S_I Soluble nonbiodegradable COD

S_S Soluble biodegradable COD

S_{ND} Biodegradable organic soluble nitrogen

S_{NH} Ammonia nitrogen

S_{NO} Nitrate

S_O Oxygen

$ts^{outflux}_{n,t}, ts^{influx}_{n,t}$ Time series parameter of exogenous flows from or to a node in Backbone

$u \in U$ Unit in Backbone

V Tank volume $[m^3]$

$v^{flowGen}_{n,u,q,t}$ Product variable of $v^{gen}_{n,u,t}$ and $q_{q,t}$ of a unit in Backbone

$v^{flowState}_{n,q,t}$ Product variable of $v^{state}_{n,t}$ and $q_{q,t}$ of a unit in Backbone

$v^{fuelCost}$ Fuel cost variable in Backbone

$v^{gen}_{n,u,t}$ Generation (consumption) variable of a unit in Backbone

v^{obj} Value of the objective function in Backbone

$v^{penalty}$ Penalty cost variable in Backbone

$v^{rampCost}$ Ramp cost variable in Backbone

$v^{shutdownCost}$ Shutdown cost variable in Backbone

$v^{spill}_{n,t}$ Spill variable of a node in Backbone

$v^{startupCost}$ Start up cost variable in Backbone

$v^{state}_{n,t}$ State variable of a node in Backbone

$v^{transfer}_{n,t}$ Transfer variable between nodes in Backbone

$v^{vomCost}$ Variable OM cost in Backbone

w_j Linearisation parameter vector for the airflow of the linear model

X Microorganism population $[g/m^3]$

X^{eff} Effluent microorganism population $[g/m^3]$

X_I and X_P Particulate nonbiodegradable COD

X_S Particulate biodegradable COD

$X_{B,A}$ Autotroph active biomass

$X_{B,H}$ Heterotroph active biomass

X_{ND} Biodegradable organic particulate nitrogen

Y_A Growth rate of autotrophs [g cell COD formed (g N oxidized)^1]

Y_H Growth rate of heterotrophs [g cell COD formed (g COD oxidized)^1]

$Z_{i,q}$ Linearisation parameter matrix for the kinetics of the linear model

AD Anaerobic digestion

ASM1 Activated Sludge Model No. 1

bCOD biodegradable Chemical Oxygen Demand

BOD Biological oxygen demand

BSM1 Benchmark Simulation Model 1

CO2 Carbon dioxide

COD Chemical Oxygen Demand

DO dissolved oxygen

DR Demand response

hsc Half-saturation coefficient

kLa Oxygen transfer coefficient [d^{-1}]

LP Linear program

MILP mixed-integer linear program

OM Operations and maintenance

PE Population Equivalent

PV Photo voltaic

SSE Sum of squared errors

TKN Total Kjeldahl Nitrogen

WWTP Wastewater treatment plant

1 Introduction

Case studies have shown the potential of wastewater treatment plants (WWTP) to provide demand response (DR) to the power system, for example by shutting down the aeration of the activated sludge process for a limited amount of time (Berger et al., 2011; Kollmann et al., 2013; Nowak et al., 2015; Schäfer et al., 2017; Müller & Möst, 2018; Giberti et al., 2019). So far, these studies have assumed power system operation and energy prices as exogenous to the demand response of WWTP. Instead, the inclusion of the WWTP operation into the energy system optimisation can yield a more holistic system perspective of large-scale DR provision by WWTP. However, wastewater treatment plant models are often characterised by a high level of complexity and non-linearity, while most power system models are (mixed-integer) linear optimisation problems. An optimisation problem that simultaneously considers both power system and wastewater treatment plant requires an integrated modelling approach that does not exist to date. We overcome this limitation by introducing a linearised reduced-order model for the activated sludge process, the core process within biological wastewater treatment, which can be integrated into a mixed-integer linear program (MILP). Starting from the Activated Sludge Model No. 1 (ASM1), a well established standard model in the realm of wastewater treatment modelling, we derive a linearised reduced-order WWTP model in three steps. First, the standard ASM1 is reduced to a non-linear three-component model. By observing only three state variables (namely, substrate concentration, biomass concentration and dissolved oxygen concentration) we can significantly reduce the complexity of ASM1. Second, we derive a set of locally valid linear models from this by using a linearisation approach introduced by Smets et al. (2006). The approach uses weighted linear combinations of the state variables for different ranges of influent flow. Depending on the level of influent, the parameters within the model change according to the respective dynamics, resulting in a distinct linear model for each range of influent flow. Third, the balance equations of the WWTP model are linearised with the help of binary variables in order to fit the MILP structure. This allows for switching between the coefficients according to the influent category.

To date, there have been various approaches to reduce the complexity of the ASM1 in the literature. Zhao et al. (1995) provide one of the first examples of model complexity reduction of the ASM1, proposing a model that only observes the state variables for the ammonia and nitrate concentrations for an alternating activated sludge process. Jeppson (1996) also develops a reduced-order model which contains the four state variables of nitrate, ammonia, biomass and COD. Similar to these first approaches, Julien et al. (1999) introduce a reduced-order model for a single tank set-up with alternating aerobic and anoxic conditions, which contains one sub-model for aerobic conditions and one for anoxic conditions. The model contains three state variables: the concentrations of nitrate, ammonia and oxygen. Mulas et al. (2007) develop a four-state variables model for oxygen, nitrate and nitrite nitrogen, free and ionised ammonia, and a reduced variable for COD, which contains the soluble organics and biodegradable particulates $S_I + S_S + X_S$. Most recently, Lahdhiri et al. (2020) discussed a model with more detail, reducing

the number of state variables from 13 in the ASM1 to 9. The approach is based on the steady-state mass balances of the ASM1 and applied to a plant layout with a single aerated tank, with sludge recycling from a subsequent settling tank. Some nonlinear reduced-order models also incorporate linear elements. The reduced-order model by Nelson et al. (2018) contains four process equations for the change of soluble substrate, particulate (heterotroph) biomass, soluble micro-pollutants and particulate micro-pollutants. They partly linearise the model, using a linear process for the adsorption of particulates by the biomass. Santa Cruz et al. (2016) identify reaction invariants within a batch system, which are unaffected by the reaction process and can be expressed as linear algebraic expressions. In three case studies, they use one, three and five reaction invariants in order to reduce the number of differential equations of the ASM1.

In addition to these reduced-order models, there have also been several examples of model linearisation of the ASM1. Smets et al. (2006) propose a relatively simple, general approach to linearise the full ASM1 model. They argue that instead of using a classic Taylor expansion, an approach with weighted linear combinations of the state variables yields a comparably good fit of the linear model. Benhalla et al. (2010) also provide a linear model for the full ASM1. Instead of the mass balances, they linearise the reaction rates by using linear combinations of state variables as well. After identification, these linear rate models are incorporated into the mass balance equations of the ASM1.

Other linearisation approaches also consider a model complexity reduction before linearisation. A two-phase model with 8 state variables for an intermittent aerobic-anoxic activated sludge process is presented by Anderson et al. (2000). The nonlinear terms within the process equations of the ASM1 are replaced by linear approximations. The model uses first-order expressions for the reaction rates in each phase (aerobic and anoxic). They highlight that the resulting model is system-specific, and might not reflect the behaviour of a different activated sludge system under different operating conditions. Gómez-Quintero et al. (2004) also present a linear model with two sub-models for the aerobic and anoxic phase of a continuous flow process. Their model contains four equations, which determine the states of the readily biodegradable substrate, nitrate, ammonia and dissolved oxygen. They find that the linear dynamics defined for the dissolved oxygen are slower compared to the ASM1, but demonstrate an overall good fit of the model under different operating conditions. David et al. (2007) develop a reduced and linearised version of the ASM1 for robust control purposes of a two-tank plant layout. Their approach is similar to a classic Taylor expansion, but instead of using steady-state points, they linearise the model for the average values of the input and state variables. This results in a linear model with five state variables for the anoxic tank and six state variables for the aerobic tank. Nagy et al. (2009) propose a multi-model approach with eight time-invariant sub-models and a set of weighting functions to combine them into a global linear model. Their reduced-order model only considers carbon pollution, but the methodology could potentially be applied to the full ASM1 as well.

In contrast to existing linearised models, our biochemical model provided the potential to be integrated into an energy systems model to understand the implications of (industrial) process constraints for demand response actions for both the power system operator and the plant operator.

2 Methodology

The full ASM1 model takes into account 13 different state variables and eight process equations in order to describe the dynamic behaviour of the wastewater components in the activated sludge process. A full representation of the ASM1 can be found in Henze et al. (1987) and Jeppson (1996). A detailed description of its successors ASM2 and ASM3 can be found in Henze et al. (2000).

The ASM1 describes the dynamics of the activated sludge process using four state variables for the nitrogen components, one for the dissolved oxygen, one for alkalinity and seven for the chemical oxygen demand (COD). COD consists of biodegradable, non-biodegradable COD and active biomass. It distinguishes between soluble (S_S) and particulate (X_S) biodegradable COD, soluble (S_I) and particulate (X_I and X_P) non-biodegradable COD. The active biomass consists of heterotroph ($X_{B,H}$) and autotroph ($X_{B,A}$) micro-organisms.

The nitrogen components that are directly included in the model are biodegradable organic soluble (S_{ND}) and particulate (X_{ND}) nitrogen, ammonia nitrogen (S_{NH}) and nitrate (S_{NO}). The model describes four different kinds of dynamic processes: (aerobic and anoxic) growth of biomass, decay of biomass, ammonification and hydrolysis. The dynamic processes for the autotrophic and heterotrophic biomass are depicted in Figure 1. Some parallel processes for nitrogen components are omitted for conciseness: Particulate organic nitrogen (X_{ND}) is embedded in X_S and is therefore hydrolysed as well and the parts of the embedded S_{ND} in S_S is released to bulk liquid as ammonia when S_S is utilised.

On that basis, we develop a reduced-order model which observes only three state variables for a lumped substrate S, the biomass concentration X and the concentration of dissolved oxygen DO. We compare the results of this model to the results of the full ASM1 for a two-week simulation period, based on benchmark data from the well-established Benchmark Simulation Model No. 1 (BSM1). Since the models observe different state variables, it is not possible to compare the results directly. Therefore, we translate the results of both models into BOD, TKN and the oxygen consumption of the process. In order to estimate the kinetic parameters of the reduced-order model, we perform a parameter estimation that minimises the sum of squared errors between the effluent concentrations to achieve the best possible match of the results of the reduced-order model and the ASM1 results.

Subsequently, the reduced-order model with estimated kinetic parameters needs to be linearised to fit a mixed-linear optimisation framework. We use the linearisation approach by Smets et al. (2006) to

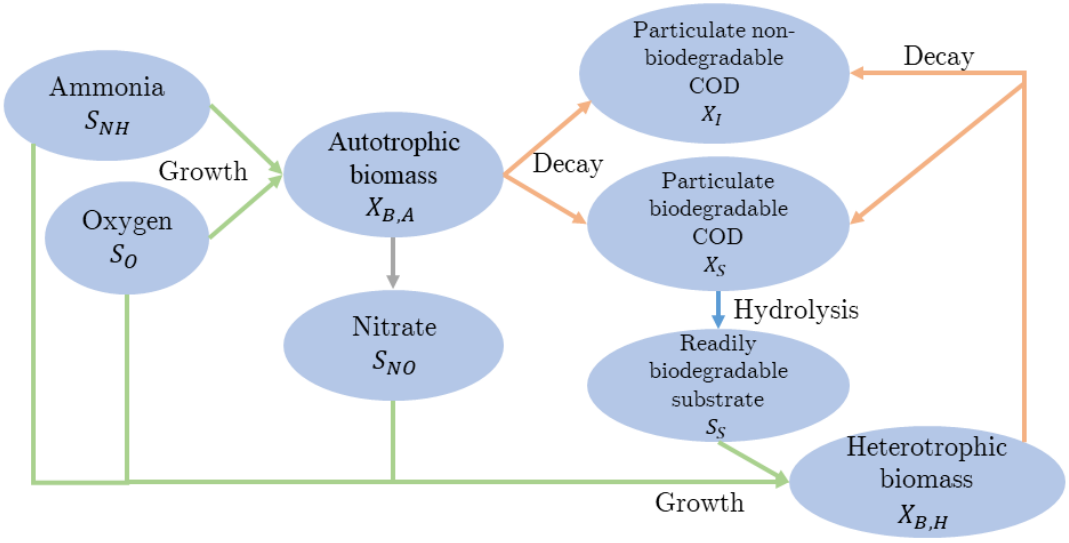

Figure 1: Dynamic processes for autotrophic and heterotrophic biomass in the ASM1

develop a linear model of the activated sludge process with the same kinetic parameters and state variables as the nonlinear reduced-order model. It consists of linear combinations of the state variables and their average values over the simulation period, weighted with a linearisation parameter that varies depending on the influent flow rate. We estimate the linearisation parameters for every inflow category such that the results of the nonlinear model match the results of the linear model. Figure 2 summarizes the model reduction process.

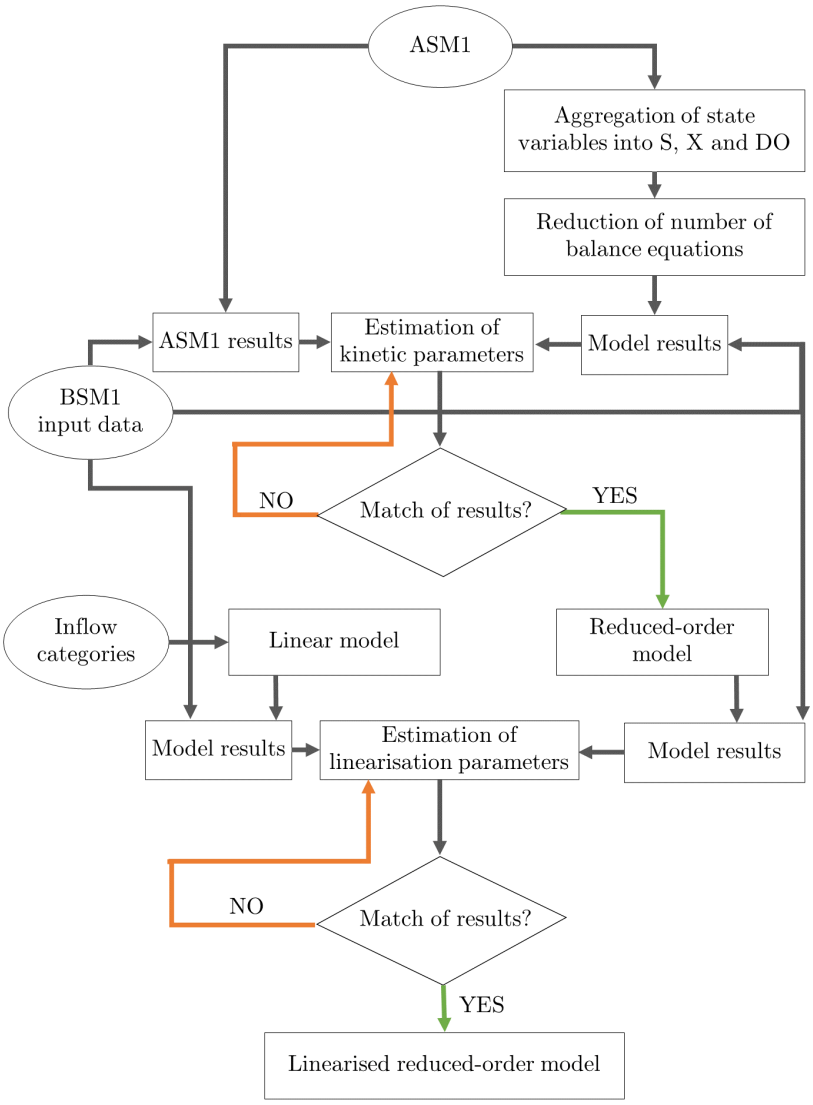

Figure 2: Model reduction process

2.1 The nonlinear reduced-order model

The simplest description of the processes involved in wastewater treatment is given in equations 1, 2 and 3. These mass balances are written considering a continuous stirred tank reactor, and illustrate the relationships between the microorganisms concentration X, the dissolved oxygen concentration DO and the concentration of the substrate S from which the microorganisms obtain the carbon and nutrients they need.

$$\frac{dS}{dt} = \frac{Q}{V} \cdot (S^{in} - S) + r_S(S, X, DO) \tag{1}$$

$$\frac{dX}{dt} = \frac{Q}{V} \cdot (X^{in} - X) + r_X(S, X, DO) \tag{2}$$

$$\frac{dDO}{dt} = \frac{Q}{V} \cdot (DO^{in} - DO) + OTR + r_S(S, X, DO) \tag{3}$$

In each equation, the first term represents the contribution of the mass fluxes that enter and leave the system, under the assumption that the liquid volume in the tank remains constant. The terms r_s, rx and r_{DO} represent the reaction rates of each state variable, whereas OTR (Oxygen transfer rate) accounts for the oxygen that is provided to the liquid phase through the aeration system.

We use this basic kinetic model as the starting point to build the reduced-order model. We consider only biodegradable carbonaceous COD, because non-biodegradable COD is assumed to be unaffected by the biochemical processes described in the ASM1. Moreover, we consider carbon matter as a fraction α of the total substrate S that is available for the microorganisms (equation 4). This accounts for both the readily biodegradable carbon (S_S) and the particulate biodegradable carbon (X_S), although its hydrolysis is neglected. The remaining substrate $(1-\alpha)S$ consists of nitrogen compounds, which ASM1 divides into ammonium and ammonia nitrogen (S_{NH}), soluble biodegradable organic nitrogen (S_{ND}), and particulate biodegradable organic nitrogen (X_{ND}). To maintain dimensional consistency while lumping carbon and nitrogen compounds in the same state variable, it is necessary to take into account the stoichiometric factor 4.57 gCOD/gN (equation 5).

$$\alpha \cdot S = S_S + X_S \tag{4}$$

$$(1-\alpha) \cdot S = (S_{NH} + S_{ND} + X_{ND}) \cdot 4.57\ gCOD/gN \tag{5}$$

The biochemical reactions that consume carbon and nitrogen compounds are characterised by different reaction rates. In particular, nitrogen removal by autotrophic biomass requires a significantly longer time than the removal of carbon. Therefore, the model should be capable of differentiating between carbon and nitrogen substrates. Moreover, the ratio between carbon and nitrogen compounds in the liquid phase is not constant, and can change substantially as the water flows through the WWTP. Hence, two α factors are considered: the first one (α_1) takes into account the carbon share in the plant influent, whereas the second (α_2) describes the carbon share in the reactor. These factors were calculated by averaging the dynamically changing values in the influent and effluent (Figure A.1 in Appendix A) over a 14-days simulation of BSM1.

ASM1 also distinguishes between heterotrophic biomass (X_{BH}) and autotrophic biomass (X_{BA}). These two different microbial populations can be accounted for with a single state variable X, assuming that X_{BH} constitutes a certain fraction β of X (equation 6), whereas the remainder $(1-\beta)$ represents X_{BA} (equation 7). Details on how we determine the value for β can be found in Appendix A.

$$\beta \cdot X = X_{BH} \tag{6}$$

$$(1-\beta) \cdot X = X_{BA} \tag{7}$$

The reaction rate in equations 1, 2 and 3 associated with each state variable can be express analogously to the ASM1, with some adjustments to account for stoichiometry. For instance, the substrate reaction rate is modelled on the basis of the ASM1 aerobic growth reaction rates, as shown in equation 8.

$$\begin{aligned} r_S = &- k_T \cdot \beta \cdot X \cdot \left(\frac{\alpha_2 \cdot S}{K_S + \alpha_2 \cdot S}\right) \cdot \left(\frac{DO}{K_{OH} + DO}\right) + \\ &- k_{Ta} \cdot (1-\beta) \cdot X \cdot \left(\frac{(1-\alpha_2) \cdot S}{4.57 \cdot K_{NH} + (1-\alpha_2) \cdot S}\right) \cdot \left(\frac{DO}{K_{OA} + DO}\right) + \\ &+ (1-f_P) \cdot k_d \cdot X \end{aligned} \tag{8}$$

The first term of equation 8 accounts for the carbon fraction of the substrate ($\alpha_2 \cdot S$), which is consumed through aerobic growth by the heterotrophic biomass ($\beta \cdot X$) that is present in the system. The second term of equation 8 represents the nitrogen fraction of the substrate ($(1-\alpha_2) \cdot S$), which is used by the aerobic growth of the autotrophic share ($(1-\beta) \cdot X$). The kinetic constants of the growth processes are k_T and k_{Ta}, which are calculated as the ratio between μ_H and Y_H, and μ_A and Y_A respectively. Finally, the last term describes the substrate originated by the cellular decay of both the heterotrophic and autotrophic fractions on the microorganisms. The decay coefficient k_d that is used here is the weighted combination of the ASM1 heterotrophs (b_H) and autotrophs (b_A) decay coefficients, as shown in equation 9.

$$k_d = \beta \cdot b_H + (1-\beta) \cdot b_A \tag{9}$$

In the ASM1, the biomass decay produces particulate biodegradable substrate (X_S), as well as particulate biodegradable organic nitrogen (X_{ND}). Since our reduced-order model does not distinguish between soluble and particulate compounds, we assume that the decay products directly increase the amount of substrate S available to the microorganisms. Moreover, all the kinetic and stoichiometric parameters that appear in the r_S equation are directly derived from the ASM1, to facilitate interpretability and consistency with the full ASM1.

Similarly, we obtain the reaction rates r_X and r_{DO}, reported in equation 10 and 11 respectively.

$$\begin{aligned} r_X = &k_T \cdot Y_H \cdot \beta \cdot X \cdot \left(\frac{\alpha_2 \cdot S}{K_S + \alpha_2 \cdot S}\right) \cdot \left(\frac{DO}{K_{OH} + DO}\right) + \\ &+ k_{Ta} \cdot Y_A \cdot (1-\beta) \cdot X \cdot \left(\frac{(1-\alpha_2) \cdot S}{4.57 \cdot K_{NH} + (1-\alpha_2) \cdot S}\right) \cdot \left(\frac{DO}{K_{OA} + DO}\right) + \\ &- k_d \cdot X \end{aligned} \tag{10}$$

$$
\begin{aligned}
r_{DO} = &-(1-Y_H)\cdot k_T\cdot\beta\cdot X\cdot\left(\frac{\alpha_2\cdot S}{K_S+\alpha_2\cdot S}\right)\cdot\left(\frac{DO}{K_{OH}+DO}\right)+\\
&-(4.57-Y_A)\cdot k_{Ta}\cdot(1-\beta)\cdot X\cdot\left(\frac{(1-\alpha_2)\cdot S}{4.57\cdot K_{NH}+(1-\alpha_2\cdot S}\right)\cdot\left(\frac{DO}{K_{OA}+DO}\right)
\end{aligned}
\tag{11}
$$

Additionally, the DO mass balance includes a term to account for the oxygen provided to the microorganisms through aeration (oxygen transfer rate - OTR). In ASM1, the oxygen transfer rate is defined by equation 12, which relies on the kLa factor to express the variations in the DO concentration produced by the aeration system, as well as environmental factors. The amount of oxygen that is transferred to the liquid phase in the reactors depends on the kLa coefficient and approaches zero when the dissolved oxygen concentration in the tank reaches the saturation concentration DO^{sat}.

$$
OTR = kLa\cdot(DO^{sat}-DO) \tag{12}
$$

We use the correlation proposed by Rieger et al. (2006) to model the effect of air flow rate (which is the controlled variable) on the reaction kinetics (see equation 13), neglecting the dependency of OTR on temperature, as well as the different performance of the aeration system in clean water and wastewater.

$$
OTR = \frac{OU_{20}\cdot h_{aer}}{V\cdot DO^{sat}}\cdot Q_{air}\cdot(DO^{sat}-DO) \tag{13}
$$

In terms of plant layout, the model is developed considering a single aerated tank (figure 3b). Compared to the standard design (figure 3a), the final clarifier and the return activated sludge stream are not explicitly modelled, as their presence would introduce significant non-linearities in the model. Instead, settling and underflow are described assuming that a constant share of biomass remains in the aerated tank.

To simulate the biomass retention without explicitly modeling the final clarifier, we introduced the efficiency factor η_X for capturing solids to the simplified model. Therefore only a fraction of the biomass leaves the system with the effluent (equation 14).

$$
X^{out} = \eta_X\cdot X \tag{14}
$$

Meanwhile, we assume that S and DO are completely soluble in the liquid phase, which means that their concentration in the plant effluent is not affected by the presence of the settler. However, the simulated recycle flow contains a certain quantity of both substrate and dissolved oxygen, and to eliminate

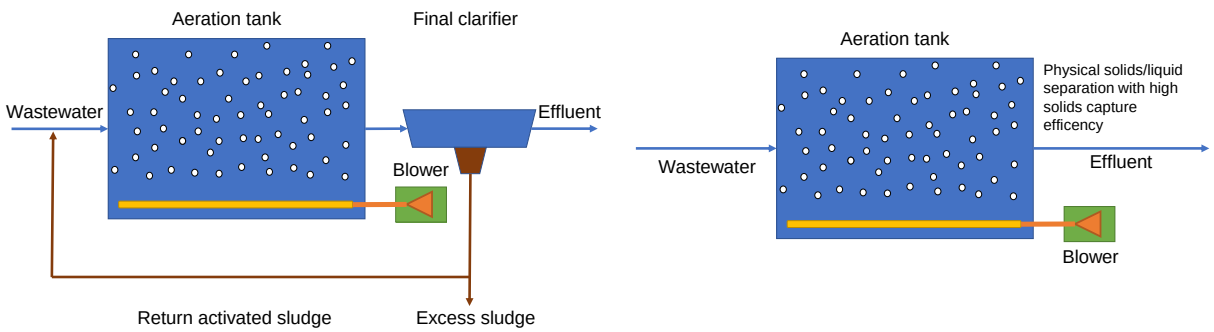

(a) Standard activated sludge layout with final clarifier

(b) Single-tank layout with implied settling and recirculation flow

Figure 3: Comparison of standard tank layout and single-tank layout

this stream from the plant layout may have repercussions on the model results. Due to the fast consumption rate of the substrate, the effect is negligible for the effluent substrate concentration. In contrast, the decreased amount of oxygen that reaches the tank due to the lack of recycling flow results in a higher expected aeration demand for the plant. To address this issue, an additional parameter γ_{DO} is introduced in the DO mass balance equation, estimating its value to match the DO concentration in the tank. This parameter is only necessary to ensure that the results of the reduced order model and the reference model are comparable: in practice, the biochemical reactions that take place in the final clarifier would deplete the oxygen in the recycle flow. Equations 15, 16 and 17 report the final mass balances of the reduced-order model.

$$\begin{aligned}\frac{dS}{dt} = &\frac{Q}{V}\cdot\frac{1+3.57\cdot\alpha_1}{4.57}\cdot(S^{in}-S)+\\ &-k_T\cdot\beta\cdot X\cdot\left(\frac{\alpha_2\cdot S}{K_S+\alpha_2\cdot S}\right)\cdot\left(\frac{DO}{K_{OH}+DO}\right)+\\ &-k_{Ta}\cdot(1-\beta)\cdot X\cdot\left(\frac{(1-\alpha_2)\cdot S}{4.57\cdot K_{NH}+(1-\alpha_2)\cdot S}\right)\cdot\left(\frac{DO}{K_{OA}+DO}\right)+\\ &+(1-f_P)\cdot k_d\cdot X\end{aligned} \tag{15}$$

$$\begin{aligned}\frac{dX}{dt} =& \frac{Q}{V} \cdot (X^{in} - \eta_X \cdot X) + \\ &+ k_T \cdot \beta \cdot X \cdot Y_H \cdot \left(\frac{\alpha_2 \cdot S}{K_S + \alpha_2 \cdot S}\right) \cdot \left(\frac{DO}{K_{OH} + DO}\right) + \\ &+ k_{Ta} \cdot (1-\beta) \cdot X \cdot Y_A \cdot \left(\frac{(1-\alpha_2) \cdot S}{4.57 \cdot K_{NH} + (1-\alpha_2 \cdot S}\right) \cdot \left(\frac{DO}{K_{OA} + DO}\right) + \\ &- k_d \cdot X\end{aligned} \tag{16}$$

$$\begin{aligned}\frac{dDO}{dt} =& \frac{Q}{V} \cdot (\gamma_{DO} \cdot DO + DO^{in} - DO) + \\ &+ \frac{OU_{20} \cdot h}{V \cdot DO^{sat}} \cdot Q_{air} \cdot (DO^{sat} - DO) + \\ &- (1 - Y_H) \cdot k_T \cdot \beta \cdot X \cdot \left(\frac{\alpha_2 \cdot S}{K_S + \alpha_2 \cdot S}\right) \cdot \left(\frac{DO}{K_{OH} + DO}\right) + \\ &- (4.57 - Y_A) \cdot k_{Ta} \cdot (1-\beta) \cdot X \cdot \left(\frac{(1-\alpha_2) \cdot S}{4.57 \cdot K_{NH} + (1-\alpha_2) \cdot S}\right) \cdot \left(\frac{DO}{K_{OA} + DO}\right)\end{aligned} \tag{17}$$

2.2 The linear reduced-order model

In the following, we linearise the equations 15, 16 and 17. Instead of a classic Taylor series expansion, a simplified linearisation technique introduced by Smets et al. (2006) is applied. They use weighted linear combinations of the state variables to approximate the nonlinear system. The approach produces similar results for the aerated tank compared to the Taylor series expansion, but provides improved modelling of peak concentrations and a reduction of complexity (Smets et al., 2006).

The idea at the base of this approach is to utilise the average values of observable state variables over a fixed simulation period in order to approximate interactions between state variables. We first apply this to the dilution factor Q/V and the kinetic parameters of the model, such that

$$\frac{\overline{Q}}{V} = \widetilde{D} \tag{18}$$

$$\frac{k_T}{(K_S + \alpha_2 \overline{S})(K_{OH} + \overline{DO})} = \delta \tag{19}$$

$$\frac{k_T a}{(4.57 K_{NH} + (1-\alpha_2)\overline{S})(K_{OA} + \overline{DO})} = \theta \tag{20}$$

All over-lined characters represent the average values of the state variable over the simulation period. Inserting equations 18, 19, 20 into the system of balance equations yields

$$\frac{dS}{dt} = \widetilde{D} \cdot \frac{1+3.57\alpha_1}{4.57} \cdot (S_{in} - S) - \delta\alpha_2\beta \cdot S \cdot DO \cdot X \\ - \theta(1-\alpha_2)(1-\beta)S \cdot DO \cdot X + (1-f_P) \cdot k_d \cdot X \tag{21}$$

$$\frac{dX}{dt} = \widetilde{D} \cdot (X_{in} - \eta_X X) + \delta\alpha_2\beta Y_H \cdot S \cdot DO \cdot X \\ + \theta(1-\alpha_2)(1-\beta)Y_A \cdot S \cdot DO \cdot X - k_d \cdot X \tag{22}$$

$$\frac{dDO}{dt} = \widetilde{D} \cdot (DO_{in} - (1-\gamma_{DO})DO) + \frac{OU_{20} \cdot h}{V \cdot DO^{sat}} \cdot Air \cdot D^{sat} - \frac{OU_{20} \cdot h}{V \cdot DO^{sat}} \cdot Air \cdot DO \\ - \delta\alpha_2\beta(1-Y_H) \cdot S \cdot DO \cdot X - \theta(1-\alpha_2)(1-\beta)(4.57-Y_A) \cdot S \cdot DO \cdot X \tag{23}$$

Subsequently, we linearise the non-linear interaction between the state variables following Smets et al. (2006), who approximate the product of the state variables S, X and DO according to equation 24.

$$S \cdot DO \cdot X \approx z_1\overline{SX} \cdot DO + z_2\overline{XDO} \cdot S + z_3\overline{DOS} \cdot X \tag{24}$$

Here, the over-lined characters represent the average values of the state variables over the full simulation period, while z_i are adjustment parameters. These adjustment or linearisation parameters are later estimated in order to fit the results of the non-linear model. In the DO mass balance, the product of the airflow Air and DO also requires linearisation. Following the approach by Smets et al. (2006), we introduce two additional adjustment parameters w_1 and w_2.

$$Air \cdot DO \approx w_1\overline{DO} \cdot Air + w_2\overline{Air} \cdot DO \tag{25}$$

Replacing all products of state variables according to this approach and rearranging the terms yields the linear formulations of the mass balances (equations 26 to 28).

$$\frac{dS}{dt} = \widetilde{D_q} \cdot \frac{1+3.57\alpha_1}{4.57} \cdot S_{in,t}$$
$$- (\alpha_2\beta\delta + \theta(1-\alpha_2)(1-\beta))z_{1,q}\overline{XS} \cdot DO_t$$
$$- (\alpha_2\beta\delta + \theta(1-\alpha_2)(1-\beta))z_{2,q}\overline{XDO} \cdot S_t$$
$$- (\alpha_2\beta\delta + \theta(1-\alpha_2)(1-\beta))z_{3,q}\overline{DOS} \cdot X_t$$
$$+ (1-f_P) \cdot k_d \cdot X_t$$
$$- \widetilde{D_q} \cdot \frac{1+3.57\alpha_1}{4.57} \cdot S_t \quad (26)$$

$$\frac{dX}{dt} = \widetilde{D_q} \cdot X_{in,t}$$
$$+ (\alpha_2\beta\delta Y_H + Y_A\theta(1-\alpha_2)(1-\beta))z_{4,q}\overline{XS} \cdot DO_t$$
$$+ (\alpha_2\beta\delta Y_H + Y_A\theta(1-\alpha_2)(1-\beta))z_{5,q}\overline{DOX} \cdot S_t$$
$$+ (\alpha_2\beta\delta Y_H + Y_A\theta(1-\alpha_2)(1-\beta))z_{6,q}\overline{SDO} \cdot X_t$$
$$- k_d \cdot X_t$$
$$- \widetilde{D_q} \cdot \eta_X X_t \quad (27)$$

$$\frac{dDO}{dt} = \widetilde{D_q} \cdot DO_{in,t}$$
$$- (\alpha_2\beta\delta(1-Y_H) + (4.57-Y_A)\theta(1-\alpha_2)(1-\beta))z_{7,q}\overline{XS} \cdot DO_t$$
$$- (\alpha_2\beta\delta(1-Y_H) + (4.57-Y_A)\theta(1-\alpha_2)(1-\beta))z_{8,q}\overline{XDO} \cdot S_t$$
$$- (\alpha_2\beta\delta(1-Y_H) + (4.57-Y_A)\theta(1-\alpha_2)(1-\beta))z_{9,q}\overline{SDO} \cdot X_t$$
$$- \frac{OU_{20} \cdot h}{V \cdot DO^{sat}} w_{1,q}\overline{Air} \cdot DO_t$$
$$+ (\frac{OU_{20} \cdot h}{V} - \frac{OU_{20} \cdot h}{V \cdot DO^{sat}} w_{2,q}\overline{DO}) \cdot Air_t$$
$$- \widetilde{D_q} \cdot (1-\gamma_{DO})DO_t \quad (28)$$

Smets et al. (2006) define the fraction $\frac{\overline{Q}}{\overline{V}}$ as the dilution factor $\widetilde{D}$. This dilution factor and the linearisation parameters z_i are only locally valid for a certain inflow range. Consequently, the system is linear for a constant influent range q, but for a variable q, the dilution factor $\widetilde{D_q}$ and the parameters $z_{i,q}$ become integer variables. Since multiplication of variables is not possible in a mixed-integer linear program, a linear function is required to trigger the switch between these variables depending on the influent range and therefore turn them into constant coefficients within that range. Therefore, a binary variable $q_{q,t}$ is intro-

duced for each inflow segment. The balance equation 26 (exemplary, see the equivalent transformations of equations 27 and 28 in Appendix B) then becomes

$$\begin{aligned}\frac{dS}{dt} = \widetilde{D_q} \cdot q_{q,t} \cdot \frac{1+3.57\alpha_1}{4.57} \cdot S_{in,t} \\ - (\alpha_2\beta\delta + \theta(1-\alpha_2)(1-\beta))z_{1,q}\overline{XS} \cdot q_{q,t} \cdot DO_t \\ - (\alpha_2\beta\delta + \theta(1-\alpha_2)(1-\beta))z_{2,q}\overline{XDO} \cdot q_{q,t} \cdot S_t \\ - (\alpha_2\beta\delta + \theta(1-\alpha_2)(1-\beta))z_{3,q}\overline{DOS} \cdot q_{q,t} \cdot X_t \\ + (1-f_P) \cdot k_d \cdot X_t \\ - \widetilde{D_q} \cdot q_{q,t} \cdot \frac{1+3.57\alpha_1}{4.57} \cdot S_t \end{aligned} \quad (29)$$

The binary variables will be one only if the flow falls into the respective inflow range, between the lower inflow bound l_q and the upper inflow bound u_q. This is assured by the following set of constraints:

$$Q^*_{q,t} \geq l_q \cdot q_{q,t} \quad (30)$$

$$Q^*_{q,t} \leq u_q \cdot q_{q,t} \quad (31)$$

$$\sum q_{q,t} = 1 \quad (32)$$

The new variable $Q^*_{q,t} = Q_t \cdot q_{q,t}$ is the product of the continuous variables Q_t and the binary $q_{q,t}$. This product can be linearised by using the big M approach (Cococcioni & Fiaschi, 2021). Therefore, a very large number M is introduced. Then, the following constraints are implemented:

$$Q^*_{q,t} \leq q_{q,t} \cdot M \quad (33)$$

$$Q^*_{q,t} \leq Q_t \quad (34)$$

$$Q^*_{q,t} \geq Q_t - (1-q_{q,t}) \cdot M \quad (35)$$

$$Q^*_{q,t} \geq 0 \quad (36)$$

This assures that the new variable will equal Q_t if the binary variable is one, and zero if the binary variable is zero. Similarly, a new variable $S^*_{q,t} = S_t \cdot q_{q,t}$ which is limited in the same way as $Q^*_{q,t}$ is introduced for every state variable S, X and DO, following equations 37 to 40.

$$S^*_{q,t} \leq q_{q,t} \cdot M \tag{37}$$

$$S^*_{q,t} \leq S_t \tag{38}$$

$$S^*_{q,t} \geq S_t - (1 - q_{q,t}) \cdot M \tag{39}$$

$$S^*_{q,t} \geq 0 \tag{40}$$

and accordingly for X_t and DO_t and $S_{in,t}$, $X_{in,t}$ and $DO_{in,t}$.

Finally, the balance equation in 29 can be transformed into a linear form, assuming discrete time steps:

$$\begin{aligned} S_t - S_{t-1} = \sum_{q \in Q} \Bigg(& \frac{1 + 3.57\alpha_1}{4.57} \cdot \widetilde{D_q} \cdot S^*_{in,t} \\ & - (\alpha_2 \beta \delta + \theta(1-\alpha_2)(1-\beta)) \overline{X} \cdot \overline{S} \cdot z_{1,q} \cdot DO^*_{q,t} \\ & - (\alpha_2 \beta \delta + \theta(1-\alpha_2)(1-\beta)) \overline{X} \cdot \overline{DO} \cdot z_{2,q} \cdot S^*_{q,t} \\ & - (\alpha_2 \beta \delta + \theta(1-\alpha_2)(1-\beta)) \overline{DO} \cdot \overline{S} \cdot z_{3,q} \cdot X^*_{q,t} \\ & - \widetilde{D}_q \cdot \frac{1 + 3.57\alpha_1}{4.57} \cdot S^*_{q,t} \Bigg) \\ & + (1 - f_P) \cdot k_d \cdot X_t \end{aligned} \tag{41}$$

In order to arrive at a globally valid model, the parameters for the vector $\widetilde{D_q}$ and the matrix $Z_{i,q}$ have to be estimated for each inflow category q.

3 Results

3.1 Calibration results of the reduced-order model against the ASM1

In order to estimate the kinetic parameters for the reduced-order model, we compare the results of the ASM1 and the reduced-order model for a representative data set of two weeks of influent data. The influent data is obtained from the Benchmark Simulation Model No. 1 (BSM1, Alex et al. (2008)). The data set contains the instantaneous flow rate and the concentrations of each influent component of the ASM1 measured at a 15 minutes time resolution. There is a data set for dry, wet and storm weather conditions. In this study, we use the dry weather influent data, because demand response can be provided more easily, if the system is not under stress from high influent loads. The average influent flow rate is 18,446 $m^3.d^{-1}$ and the size of the aerated tank is 6000 m^3. Table 1 gives an overview of all assumed values of the model parameters, derived from the ASM1 and BSM1.

Parameter	symbol	unit	value
Average flow rate	$\overline{Q}$	$m^3.d^{-1}$	18,446
Average airflow rate	$\overline{Air}$	$m^3.d^{-1}$	144,000
Tank volume	V	m^3	6000
Initial DO concentration	DO_0	g/m^3	0.0076964
Initial substrate concentration	S_0	g/m^3	190.37
Initial biomass concentration	X_0	g/m^3	2703.78
DO saturation concentration	DO^{sat}	g/m^3	8.00
Fraction of biomass yielding particulate products	f_P	no dimension	0.08
Immersion depth of diffusers in aerated tank	h	m	4.00
Oxygen utilisation rate	OU_{20}	$g/(m^3 \cdot m)$	20
Nitrogen content in biomass	i_{XB}	g N	0.086
Nitrogen content in products from biomass	i_{XP}	g N	0.06
Ammonification rate	k_a	m^3 (g COD day)$^{-1}$	0.08
Max. specific hydrolysis rate	k_h	g slowly biodeg. COD (g cell COD day)$^{-1}$	3.0
Ammonia half-saturation coefficient for autotrophs	K_{NH}	g $NH_3 - Nm^{-3}$	1.0
Nitrate half-saturation coefficient for denitrifying heterotrophs	K_{NO}	g NO_3-N m^{-3}	0.5
Oxygen half-saturation coefficient for autotrophs	K_{OA}	g O_2 m^{-3}	0.4
Half-saturation coefficient for heterotrophs	K_S	g COD m^{-3}	10.0
Half-saturation coefficient for hydrolysis of slowly biodegradable substrate	K_X	g slowly biodeg. COD (g cell COD)$^{-1}$	0.1
Oxygen transfer coefficient	kLa	d^{-1}	240
Oxygen half-saturation coefficient for heterotrophs	K_{OH}	g O_2 m^{-3}	0.2
Heterotrophic yield	Y_H	g cell COD formed (g COD oxidized)$^{-1}$	0.67
Autotrophic yield	Y_A	g cell COD formed (g N oxidized)$^{-1}$	0.24

Table 1: Parameter values of the linear reduced-order model, based on the ASM1 and BSM1

As stated before, the reduced-order model consists of lumped state variables for the substrate S and the microorganisms X. In order to compare the results with the results of the ASM1, the observed state variables of both models are expressed as BOD, TKN and dissolved oxygen consumption DO^{con}. In the ASM1, BOD, TKN and DO consumption are defined as:

$$BOD = 0.25 \cdot (S_S^{out} + X_S^{out} + (1 - f_P) \cdot (X_{B,H}^{out} + X_{B,A}^{out})) \tag{42}$$

$$TKN = S_{NH}^{out} + S_{ND}^{out} + X_{ND}^{out} + i_{XB} \cdot (X_{B,H}^{out} + X_{B,A}^{out}) \tag{43}$$

$$DO^{con} = \frac{Q^{in}}{V} \cdot (S_O^{in} - S_O^{out}) + kLa \cdot (DO^{sat} - S_O^{out}) - dDO \tag{44}$$

In comparison, BOD, TKN and DO consumption in the reduced-order model are given as:

$$BOD = 0.25 \cdot (\alpha_2 \cdot S + (1 - f_P) \cdot X) \tag{45}$$

$$TKN = ((1 - \alpha_2) \cdot S)/4.57 + i_{XB} \cdot X \tag{46}$$

$$DO^{con} = \frac{Q}{V} \cdot (DO_{in} - DO) + \frac{OU \cdot h}{V \cdot DO^{sat}} \cdot Air \cdot (DO^{sat} - DO) - dDO \tag{47}$$

The BOD formulation of the reduced-order model combines the organic carbon components S^S and X^S into the organic fraction of the substrate αS (see Equation 4). In the reduced-order model, the concentration of microorganisms X represents both heterotrophs and autotrophs, such that $X = X_{B,H} + X_{B,A}$.

Following equation 46, the TKN calculation consists of the nitrogenous part of S, $(1-\alpha)S$ and the nitrogen content in the effluent biomass $i_{XB}X$. For these terms to be added up, the nitrogen concentration has to be expressed in oxygen terms: 4.57 g oxygen is required to convert 1 g of ammonium nitrogen to nitrate nitrogen. The DO consumption of the process is defined by the difference of the DO concentration in the influent and the effluent, plus the additional DO supply by the aeration system, minus the change in DO concentration in the reaction tank.

The parameters μ_A, μ_H, b_H, b_A, α_1, α_2, β, η_X and γ_{DO} of the reduced-order model are estimated by minimising the sum of squared errors (SSE) between the results for the DO consumption, BOD and TKN concentration of the ASM1 and of the reduced-order model. We perform the parameter estimation using the Simulink Toolbox of the MATLAB software by The MathWorks, Inc. First, the software produces a reference signal $y_{ref}(t)$ from the ASM1 for each component. Second, a simulated signal $y_{sim}(t)$ for the reduced-order model is obtained based on a certain starting value for the parameters. For the parameters derived from the ASM1, we chose the ASM1 values as starting points for the estimation. For the new parameters α_1, α_2, β, η_X and γ_{DO}, we select a starting value of 0.5. Then, we perform the parameter estimation with the nonlinear least squares method, minimising the sum of squared errors $F(x)$ between the model prediction $y_{sim}(t)$ and the reference values $y_{ref}(t)$ using a trust-region reflective algorithm (equations 48 and 49).

$$min\, F(x) = \sum_{t=0}^{t_N} e(t) \times e(t) \;\; , with \tag{48}$$

$$e(t) = y_{ref}(t) - y_{sim}(t) \tag{49}$$

The results for dissolved oxygen consumption, BOD and TKN of the effluent of the ASM1 compared to the reduced-order model with estimated kinetic parameters are depicted in figure 4. The estimated parameter values for the reduced-order model are given in table 2.

It can be seen in figure 4 that the reduced-order model is able to predict the *DO* consumption of the process fairly accurate compared to the ASM1, although the DO consumption is slightly overestimated in the valleys.

The differences in the prediction of BOD in the effluent is caused by the different dynamics that the presence of the settler introduces to the model. The reduced-order model does not account for particulates in the substrate, since the substrate is assumed to be fully soluble. Consequently, the ASM1 can predict changes in the effluent BOD due to the degradation of particulate substrate, which the reduced-order model cannot account for. However, the average BOD in the effluent is similar in both models and the deviations from the full ASM1 behaviour remain within ± 1 g/m3, which is not so different from the sensitivity of a typical BOD5 measurement.

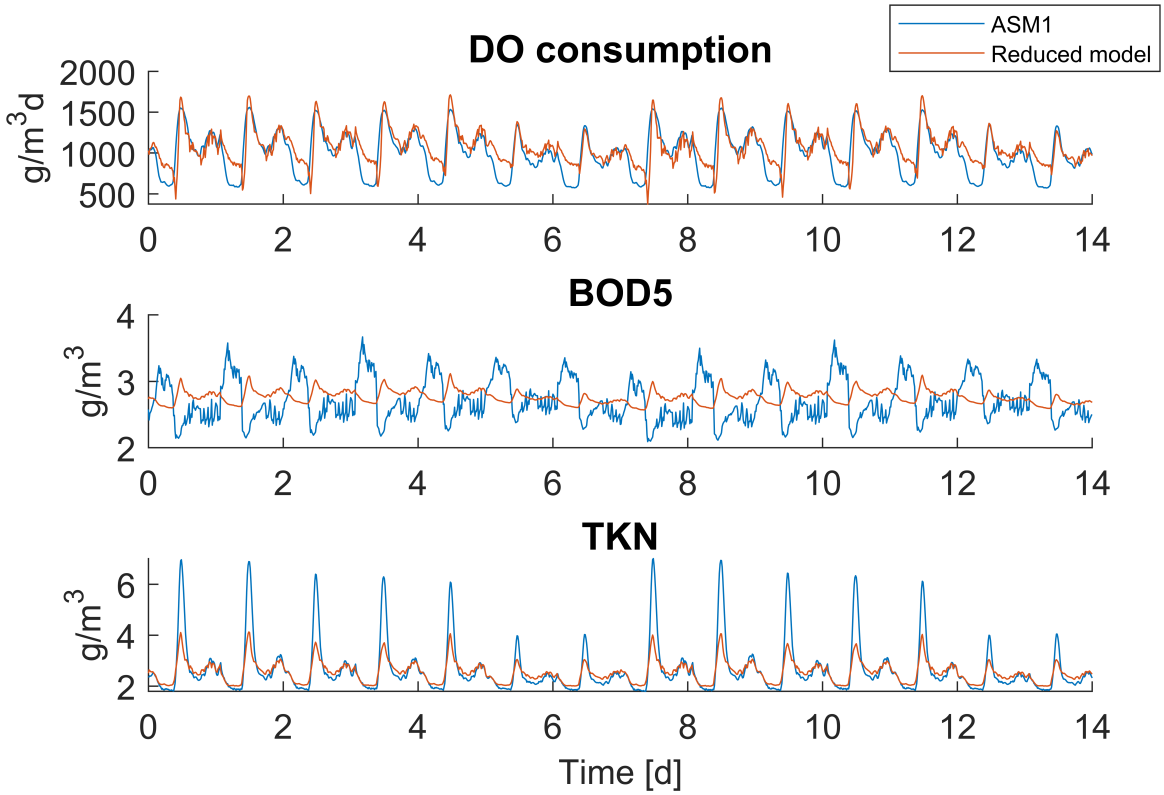

Figure 4: Effluent results of the reduced-order model against the ASM1

The baseline and dynamics of the TKN concentration in the effluent are captured well by the reduced-order model. However, the model structurally underestimates nitrogen peaks. This is because the reduced-order model does not fully capture the concentration of ammonia in the effluent, which is the main driver of nitrogen peaks in the ASM1.

Overall, these results show that the proposed reduced-order model retains the most important features of the full ASM1 for modelling DR from a WWTP with an activated sludge process while necessitating only three states variable.

3.2 Calibration results of the linear reduced-order model against the non-linear reduced-order model

Subsequently, we develop a Simulink implementation of the linearised mass balances illustrated in equations 26 to 28. We compare its results based on the BSM1 dry weather influent data to the results of the nonlinear reduced order model. The linearisation parameters z_i for the linear reduced-order model can then be estimated by minimising the sum of squared errors between the two models using a trust-region

Parameter	symbol	unit	BSM1	reduced-order model
Growth rate of heterotrophs	μ_H	d^{-1}	4.0	2.6202
Growth rate of autotrophs	μ_A	d^{-1}	0.5	0.4295
Decay rate of heterotrophs	b_H	d^{-1}	0.3	0.3235
Decay rate of autotrophs	b_A	d^{-1}	0.05	0.0393
Average DO concentration	DO_{ave}	g/m^3	3.5033	3.5033
Average substrate concentration	S_{ave}	g/m^3	-	9.2015
Average biomass concentration	X_{ave}	g/m^3	-	5335.35
Share of carbonaceous biodeg. substrate in influent	α_1	no dimension	-	0.55
Share of carbonaceous biodeg. substrate in tank	α_2	no dimension	-	0.1543
Share of heterotrophs in biomass	β	no dimension	-	0.9633
Share of biomass concentration in the effluent	η_X	no dimension	-	0.0019
Correction factor for re-circulation of DO	γ_{DO}	no dimension	-	48.9459

Table 2: Parameters of the ASM1 and the nonlinear reduced-order model

reflective algorithm (compare equations 48 and 49).

Each of the mass balance equations contains three linearisation parameters z_i, which means that a total of nine linearisation parameters is required to linearise the behaviour of system for each of the influent categories considered. Thus, the final number of required linearisation parameters is equal to the product of the number of linearisation parameters in each interval and the number of influent categories chosen. The number of intervals is thus critical in defining the complexity of the final linearised model: a larger number of intervals means that each sub-model is linear over a smaller range of values, which improves the results. It also implies a larger number of linearisation parameters to be estimated, which increases the overall model complexity. Conversely, choosing less intervals means that the sub-models are approximating the nonlinear system over a wider range of influent flow rate values. If this requires a smaller number of linearisation parameters, it can also mean reduced model performance. Hence, the number of intervals should be chosen looking for the best trade-off between these two competing aspects.

Multiple locally valid sub-models need to be estimated in order to obtain a globally valid model. Each sub-model linearises the system behaviour in a limited range of influent flow rate values. Thus, the first step of the process is the definition of such intervals. Dividing the influent data set into percentiles ensures the definition of categories with the same number of data points. Here, we demonstrate results for three inflow categories (low, medium and high).

With three inflow categories (low, medium and high) and a constant airflow rate, there are 9 linearisation parameters to estimate in every inflow category, making up 27 parameters to estimate in total. The limits of the inflow categories are determined based on the 0.33 and 0.66 percentiles of the influent flow rate. The upper limit of category 'low' (and lower limit of category 'medium') is 15,403 m^3/day, and the upper limit of category 'medium' (and lower limit of category 'high') is 20,439 m^3/day (see Figure C.1

in Appendix C).

We perform a robustness check for the number of inflow categories since the fit of the linearised model is likely to increase with the number of inflow categories. The respective percentiles of the inflow rate determine the thresholds of the models: 0.5-percentile for the model with two categories, 0.33 and 0.66 for three categories and percentiles 0.25, 0.5 and 0.75 for four categories. The results show that there is a trade-off between the fit of the model (measured by the SSE) and the number of parameters to be estimated (table 3). The reduction in SSE between two and three categories is substantial (42 % decrease), whereas the relative change between three and four categories is much smaller (5 % decrease). Therefore, the model with three inflow categories seems to be a good choice in order to obtain a model with a manageable number of linearisation parameters and a good fit.

Model	inflow thresholds (m^3/day)			Number of linearisation parameters	SSE
	1^{st}	2^{nd}	3^{rd}		
2 categories	17,871			18	3.96
3 categories	15,403	20,439		27	2.30
4 categories	13,225	17,871	21,698	36	2.19

Table 3: Comparison of different number of inflow categories

The estimated values of the linearisation parameters are given in table 4. While we estimate the values of the weighting matrix Z_i, the parameters w_1 and w_2 can be calculated from equations 12 and 13. For a constant airflow rate Air_t, equation D.1 yields $w_1 = Air_t/\overline{Air} = 1$ and $w_2 = 0$ (see the supplementary material for a systematic derivation).

$$\frac{(OU_{20} \cdot h_{aer})}{(V \cdot DO^{sat})} \cdot Air \cdot (DO^{sat} - DO) = kLa \cdot (DO^{sat} - DO) \tag{50}$$

Comparing the effluent results of all three models shows that the linear system with three inflow categories is able to predict the BOD, TKN and DO consumption of the nonlinear reduced-order model with very little loss of information. Peaks in the BOD and TKN concentration are slightly underestimated. However, the peaks of the DO consumption are captured well by the linearised model, which is the most important factor for predicting the energy consumption of the process accurately. The loss of accuracy mainly stems from the reduction of the model complexity rather than the linearisation of the model (figure 5). As already highlighted in figure 4, the fit of the BOD concentrations is the weakest among the three outcomes, because the model does not account for particulate substrate, unlike the ASM1. However, deviations remain small and the average BOD concentration is similar in all models. The fit of the TKN concentration is generally good, although peaks are structurally underestimated by 2 to 2.5 g/m^3.

	inflow range		
parameter	low	medium	high
z_1	0.0525	0.1145	0.0610
z_2	0.7315	0.7082	0.4231
z_3	0.1735	0.1591	0.5665
z_4	0.0001	0.1919	0.3028
z_5	0.5004	0.0046	0.4654
z_6	0.3526	0.7892	0.3739
z_7	0.0272	0.0827	0.0966
z_8	0.4541	0.3820	0.3459
z_9	0.4539	0.5070	0.5711
w_1	1	1	1
w_2	0	0	0

Table 4: Linearisation parameters of the linear reduced-order model

However, the DO consumption of the process is satisfactorily predicted both by the reduced-order model and the linearised model.

The main objective of the reduction and linearisation of the ASM1 is to obtain a realistic estimate of the DO concentration, because that is driving the energy consumption of the aeration process. Figure 6 shows that the DO concentration in the linear model matches the values of the nonlinear model well. As mentioned before, the loss of detail mainly occurs because of the reduction process, since the nonlinear reduced-order model does not capture the peaks of the DO concentration in the ASM1 in detail. However, the dynamics of the process are captured well, although the amplitude is structurally underestimated in the reduced-order model.

4 Discussion

In general, the reduced-order model and the linearised reduced-order model show a satisfactory fit to the ASM1 in terms of process dynamics. Predictions for the BOD, TKN and DO concentrations are comparable across the three models. The dynamics of the BOD concentration are different in the reduced-order models, which is a direct result of omitting particulate substrate components. However, the differences are small in scale and the average BOD concentrations are similar. The structural underestimation of peak concentrations of BOD and TKN compared to the ASM1 results in a final model which yields more conservative results for any DO control strategy. If a focus on very precise effluent quality control is desired, the model could be extended to include more processes, in particular denitrification. However, the application for an integrated energy-systems model requires first and foremost a realistic prediction of the DO consumption profile and thereby the energy consumption profile of the process. The results show that the model estimates the DO concentration and consumption of the activated sludge process

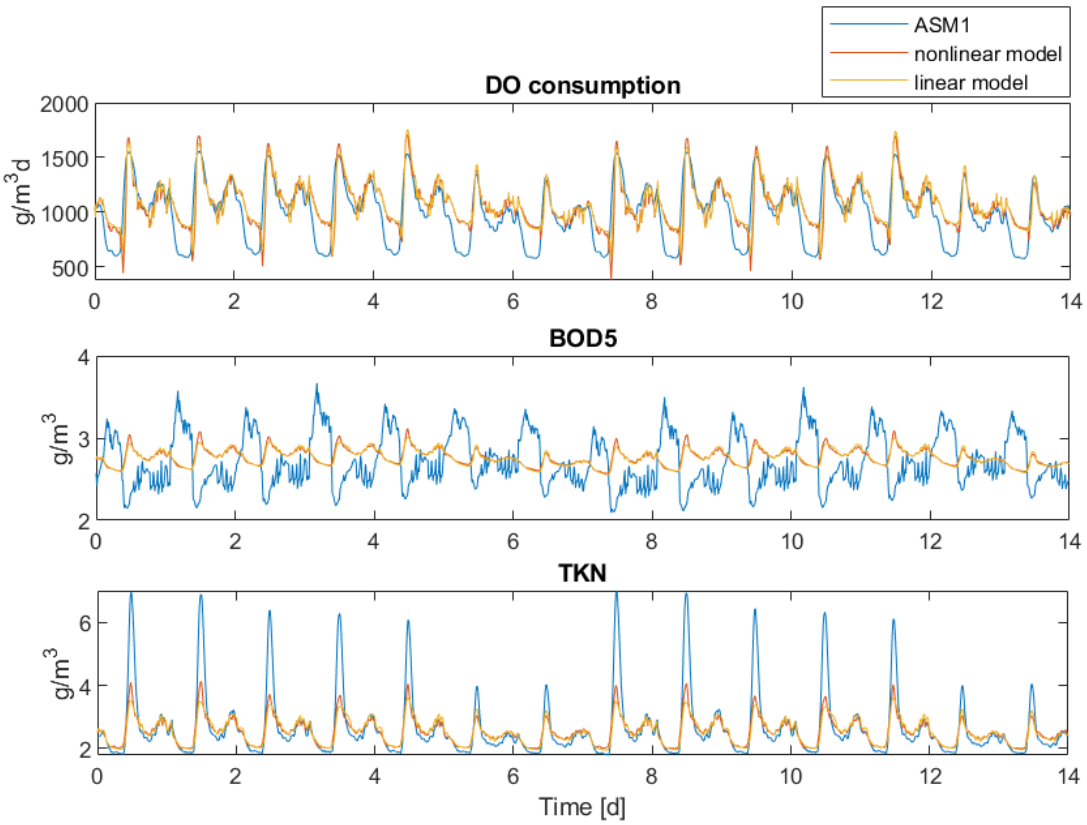

Figure 5: Effluent results of the ASM1, the reduced-order model and the linear reduced-order model compared

very well, and therefore proves to be suitable for further integrated energy-water system applications.

Since we do not model nitrate as a state variable, one limitation of the reduced-order model is the exclusion of the denitrification process. In plants with denitrification, oxygen can be recovered via this process, which reduces the aeration requirements by approximately 30 %. Consequently, the model developed in this article is applicable to plants that employ only nitrification, but overestimates the oxygen demand for plants with denitrification. That means that the energy consumption by the aeration process for these plants is likely overestimated as well. This has to be considered when applying the model to plants that also use denitrification. In the future, a more sophisticated version of the model could include the denitrification process, leading to a more accurate, but potentially more complex model.

Furthermore, the linearised reduced-order model is estimated for a constant airflow rate. Consequently, the model is only valid for average airflow rates which are similar to the applied 144,000 m^3/day. This limits the applicability of the model in times when the airflow rate is particularly high or low, or even zero. For demand response strategies, this implies that the model would yield misleading results for ef-

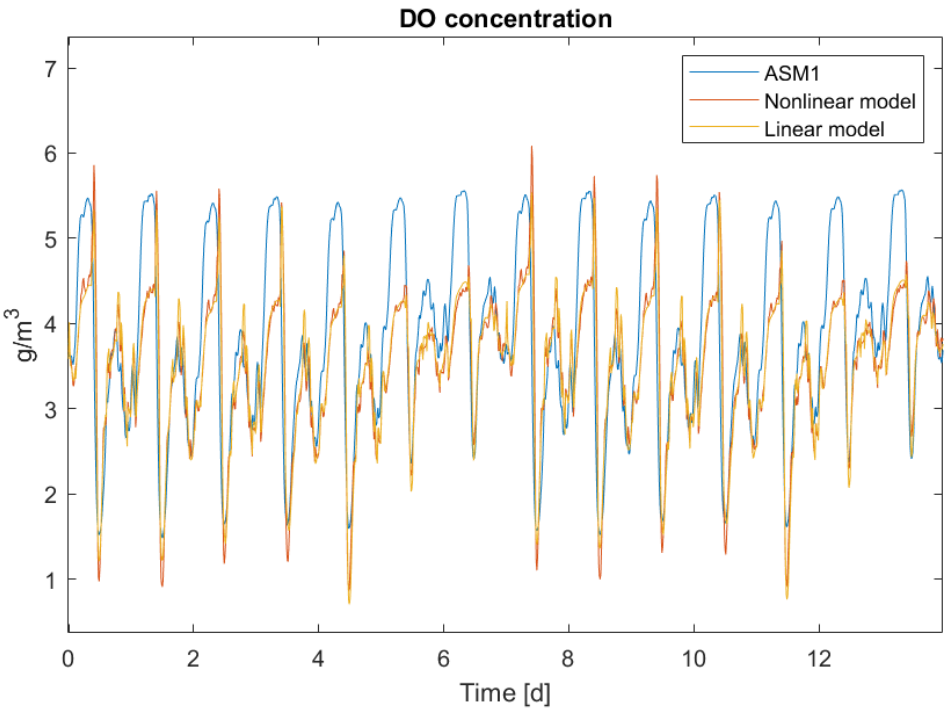

Figure 6: DO concentration of the ASM1, the reduced-order model and the linear reduced-order model compared

fluent concentrations when the aeration is shut down. Instead, the model is suitable for load shedding in a smaller range around the assumed average airflow rate. The inclusion of different airflow categories, similar to the approach taken for inflow categories, could be a future advancement of the model in order to allow for a wider range of operational flexibility of the aeration control. However, this comes with a proportional increase in linearisation parameters to be estimated and further mathematical complications within the integrated energy-systems model. An advantage of the linearised reduced-model presented here is its reduced complexity compared to the ASM1, which is why adding more complexity to the model should be well considered and justified.

Finally, the model has been estimated for a particular plant layout and specific process conditions, based on the benchmark model BSM1. The model parameters are specific to this plant model and weather conditions and would need to be re-evaluated in case of changes. However, the modelling algorithm introduced in figure 2 can easily be reapplied for a different data set in order to represent a different plant layout or different inflow conditions (for example, calibrating the model for storm weather influent conditions instead of dry weather).

5 Conclusion

Wastewater treatment process models such as the standard model ASM1 are generally characterised by a high degree of non-linearity and complexity. The aim of this paper is the complexity reduction and linearisation of such a model in order to enable its integration into a mixed-integer linear program often used in energy system modelling. Although some attempts at linearised reduced-order versions of the ASM1 have been made in the literature, this model is the first with a particular focus on the oxygen consumption and thereby the energy consumption of the process. It is also unique in its aggregation of observable state variables into only three components (substrate, biomass and oxygen), which makes it relatively simple, easily replicable for different data sets and suitable for the integration into a mixed-integer linear energy system optimisation framework. Although the model reduction leads to some model limitations, such as disregarding denitrification or variations in the airflow rate, the linear reduced-order model yields satisfactory results for the effluent concentration of BOD, TKN and the DO consumption. In particular, it captures the dynamics of the DO concentration and consumption well, which are the main predictors for the energy consumption of the aeration process.

Since the purpose of the linear reduced-order model is to provide more operational detail of the wastewater treatment process when evaluating potential demand response strategies, the next step of the research is to integrate the model as process constraints into an elaborate energy system optimisation model. The inclusion of the linear reduced-order model assures that load shedding or shifting does not lead to undesirable effects on the effluent quality and thereby provides a more realistic assessment of the flexibility potential of WWTP than traditional black-box approaches.

Future improvements of the model could include a wider representation of operational conditions, such as a more flexible variation in airflow rate, and weather conditions, such as wet and storm weather inflows. In order to represent a wider configuration of WWTPs, denitrification could be added to the model as well. In order to test the fit of the model for real-life plant conditions, the evaluation of model parameters for real WWTP data instead of benchmark data would also be a valuable task for future research.

References

Alex, J., Benedetti, L., Copp, J., Gernaey, K., Jeppsson, U., Nopens, I., ... others (2008). *Benchmark simulation model no. 1 (BSM1)* (Tech. Rep.). IWA Taskgroup on benchmarking of control strategies for WWTPs.

Anderson, J., Kim, H., McAvoy, T., & Hao, O. (2000). Control of an alternating aerobic–anoxic activated sludge system—part 1: development of a linearization-based modeling approach. *Control Engineering Practice*, *8*(3), 271–278.

Benhalla, A., Houssou, M., & Charif, M. (2010). Linearization of the full activated sludge model No 1 for interaction analysis. *Bioprocess and biosystems engineering*, *33*(6), 759–771.

Berger, H., Eisenhut, T., Polak, S., & Hinterberger, R. (2011). *Demand response potential of the Austrian industrial and commerce sector* (Tech. Rep.). Bundesministerium für Verkehr, Innovation und Technologie, Austria.

Cococcioni, M., & Fiaschi, L. (2021). The big-m method with the numerical infinite m. *Optimization Letters*, *15*(7), 2455–2468.

David, R., Wouwer, A. V., Vasel, J.-L., & Queinnec, I. (2007). Model reduction and robust control of the activated sludge process. In *2007 european control conference (ecc)* (pp. 4195–4201).

Giberti, M., Dereli, R. K., Flynn, D., & Casey, E. (2019). Predicting wastewater treatment plant performance during aeration demand shifting with a dual layer reaction settling model. *Water Science and Technology*.

Gómez-Quintero, C.-S., Queinnec, I., & Spérandio, M. (2004). A reduced linear model of an activated sludge process. *IFAC Proceedings Volumes*, *37*(3), 219–224.

Henze, M., Grady, C., Gujer, W., Marais, G., & Matsuo, T. (1987). *Activated sludge model No. 1* (Tech. Rep.). IAWQ Scientific and Technical Report No. 1.

Henze, M., Gujer, W., Mino, T., & Van Loosdrecht, M. (2000). *Activated sludge models ASM1, ASM2, ASM2d and ASM3*. IWA publishing.

Jeppson, U. (1996). *Modelling aspects of wastewater treatment processes.* Lund University.

Julien, S., Lessard, P., & Barbary, J. (1999). A reduced order model for control of a single reactor activated sludge process. *Mathematical and Computer Modelling of Dynamical Systems*, *5*(4), 337–350.

Kollmann, A., Amann, C., Elbe, C., Heinisch, V., Kraußler, A., Moser, S., ... Schmidthaler, M. (2013). Lastverschiebung in Haushalt, Industrie, Gewerbe und kommunaler Infrastruktur – Potenzialanalyse

für Smart Grids - LOADSHIFT. In *Internationale energiewirtschaftstagung an der tu wien* (pp. 1–16). .

Lahdhiri, A., Lesage, G., Hannachi, A., & Heran, M. (2020). Steady-state methodology for activated sludge model 1 (ASM1) state variable calculation in MBR. *Water*, *12*(11), 3220.

Mulas, M., Tronci, S., & Baratti, R. (2007). Development of a 4-measurable states activated sludge process model deduced from the ASM1. *IFAC Proceedings Volumes*, *40*(5), 213–218.

Müller, T., & Möst, D. (2018). Demand response potential: Available when needed? *Energy Policy*, *115*, 181–198.

Nagy, A. M., Mourot, G., Marx, B., Schutz, G., & Ragot, J. (2009). Model structure simplification of a biological reactor. *IFAC Proceedings Volumes*, *42*(10), 257–262.

Nelson, M., Alqahtani, R. T., & Hai, F. I. (2018). Mathematical modelling of the removal of organic micropollutants in the activated sludge process: a linear biodegradation model.

Nowak, O., Enderle, P., Schloffer, M., Lang, E., & Pregartbauer, R. (2015). *Loadshift-ARA - Lastverschiebung in der Abwasserreinigung - Kommunale Kläranlagen als Bestandteil smarter Energiesysteme.* (Tech. Rep.). 4ward Energy Research GmbH.

Rieger, L., Alex, J., Gujer, W., & Siegrist, H. (2006). Modelling of aeration systems at wastewater treatment plants. *Water science and technology*, *53*(4-5), 439–447.

Santa Cruz, J. A., Mussati, S. F., Scenna, N. J., Gernaey, K. V., & Mussati, M. C. (2016). Reaction invariant-based reduction of the activated sludge model ASM1 for batch applications. *Journal of environmental chemical engineering*, *4*(3), 3654–3664.

Schäfer, M., Hobus, I., & Schmitt, T. G. (2017). Energetic flexibility on wastewater treatment plants. *Water Science and Technology*, *76*(5), 1225–1233.

Smets, I., Verdickt, L., & Van Impe, J. (2006). A linear ASM1 based multi-model for activated sludge systems. *Mathematical and Computer Modelling of Dynamical Systems*, *12*(5), 489–503.

Zhao, H., Isaacs, S., Søeberg, H., & Kümmel, M. (1995). An analysis of nitrogen removal and control strategies in an alternating activated sludge process. *Water research*, *29*(2), 535–544.

Appendix A Alpha and beta factors

The value of the parameter α can be determined analysing the composition of the plant influent. Figure A.1 shows that the ratio between carbon and nitrogen compounds in the plant influent did not significantly vary from the average value ($\alpha = 0.55$) in our case study. Furthermore, all data points fall within 30% of the average value. However, the biochemical reactions that consume carbonaceous compounds are characterised by different reaction rates (e.g. nitrogen removal by autotrophic biomass requires a much longer time than the removal of carbon matter). Thus, the carbon fraction of the total substrate S may change after the treatment process, invalidating the use of a constant α factor in the reduced order model. Figure A.1 also shows the α factor calculated for the settler effluent: as expected, the fraction of carbon compounds is much lower than in the plant influent. While this suggests that one single α factor is not sufficient to properly capture the dynamics of the entire system, the variability exhibited by the α profile in the settler effluent is comparable to the one seen in the plant influent. For this reasons, two α factors are considered: the first one (α_1) takes into account the carbon share in the plant influent, whereas the second (α_2) describes the carbon share in the reactor.

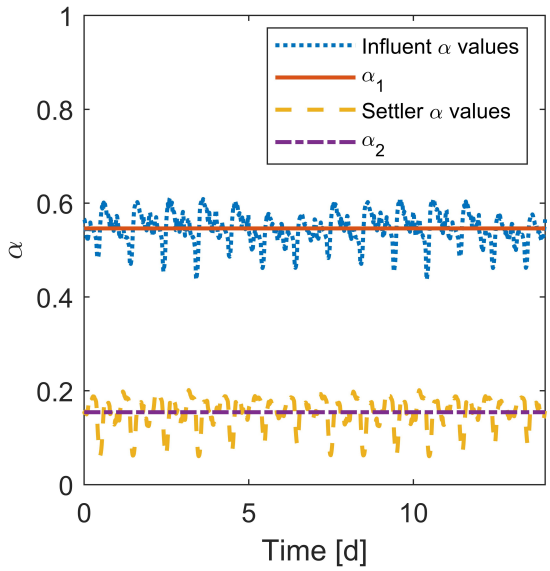

Figure A.1: Comparison between the carbon compounds fraction in the plant influent (α_1), and the carbon compounds fraction in the settler effluent (α_2).

Figure A.2 shows the β values when the ASM1 kinetics are implemented. As expected, given the slower growth rate of autotropic biomass, heterotrophs constitute the largest microorganism population in the system. Changes in microbial population generally require a long time, usually several sludge ages, when the plant is operated at stable operating conditions. As depicted in Figure A.2, the variations of the share of heterotrophic biomass in the total microorganisms concentration are even smaller than the ones

observed for α, which suggests that the use of a constant value for β is a good approximation.

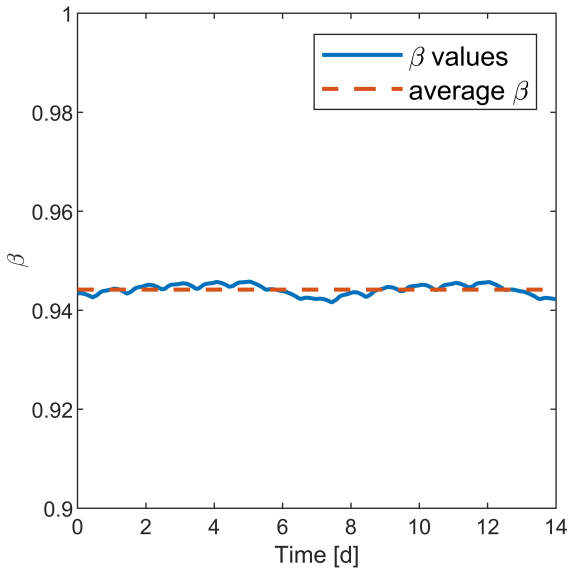

Figure A.2: Share of heterotrophic biomass in the reactor tank using ASM1 as kinetic model, and its average value.

Appendix B Transformation of balance equations

Equations B.11 and B.12 give the nonlinear reduced-order equations for the biomass concentration X and the dissolved oxygen concentration DO, including the binary flow variables:

$$\begin{aligned}\frac{dX}{dt} = \widetilde{D_q} \cdot q_{q,t} \cdot X_{in,t} \\ + (\alpha_2 \beta \delta Y_H + Y_A \theta (1-\alpha_2)(1-\beta)) z_{4,q} \overline{XS} \cdot q_{q,t} \cdot DO_t \\ + (\alpha_2 \beta \delta Y_H + Y_A \theta (1-\alpha_2)(1-\beta)) z_{5,q} \overline{DOX} \cdot q_{q,t} \cdot S_t \\ + (\alpha_2 \beta \delta Y_H + Y_A \theta (1-\alpha_2)(1-\beta)) z_{6,q} \overline{SDO} \cdot q_{q,t} \cdot X_t \\ - k_d \cdot X_t \\ - \widetilde{D_q} \cdot q_{q,t} \cdot \eta_X X_t \end{aligned} \quad \text{(B.1)}$$

$$\begin{aligned}\frac{dDO}{dt} = \widetilde{D_q} \cdot q_{q,t} \cdot DO_{in,t} \\ - (\alpha_2\beta\delta(1-Y_H) + (4.57-Y_A)\theta(1-\alpha_2)(1-\beta))z_{7,q}\overline{XS} \cdot q_{q,t} \cdot DO_t \\ - (\alpha_2\beta\delta(1-Y_H) + (4.57-Y_A)\theta(1-\alpha_2)(1-\beta))z_{8,q}\overline{XDO} \cdot q_{q,t} \cdot S_t \\ - (\alpha_2\beta\delta(1-Y_H) + (4.57-Y_A)\theta(1-\alpha_2)(1-\beta))z_{9,q}\overline{SDO} \cdot q_{q,t} \cdot X_t \\ - \frac{OU_{20} \cdot h}{V \cdot DO^{sat}} w_{1,q}\overline{Air} \cdot DO_t \\ + (\frac{OU_{20} \cdot h}{V} - \frac{OU_{20} \cdot h}{V \cdot DO^{sat}} w_{2,q}\overline{DO}) \cdot Air_t \\ - \widetilde{D_q} \cdot q_{q,t} \cdot (1-\gamma_{DO})DO_t \end{aligned} \tag{B.2}$$

In order to linearise these equations, the new variables $X^*_{q,t} = X_t \cdot q_{q,t}$ and $DO^*_{q,t} = DO_t \cdot q_{q,t}$ are introduced and constrained according to Equations B.3-B.6 and B.7-B.10:

$$X^*_{q,t} \leq q_{q,t} \cdot M \tag{B.3}$$
$$X^*_{q,t} \leq X_t \tag{B.4}$$
$$X^*_{q,t} \geq X_t - (1-q_{q,t}) \cdot M \tag{B.5}$$
$$X^*_{q,t} \geq 0 \tag{B.6}$$

$$DO^*_{q,t} \leq q_{q,t} \cdot M \tag{B.7}$$
$$DO^*_{q,t} \leq DO_t \tag{B.8}$$
$$DO^*_{q,t} \geq DO_t - (1-q_{q,t}) \cdot M \tag{B.9}$$
$$DO^*_{q,t} \geq 0 \tag{B.10}$$

Furthermore, the assumption of a constant airflow yields $w_1 = 1$ and $w_2 = 0$ (see section D). Assuming discrete time steps, the resulting set of linearised equations is:

$$
\begin{aligned}
X_t - X_{t-1} = \sum_{q \in Q} \Big(& \widetilde{D_q} \cdot X^*_{in,t} \\
& + (\alpha_2 \beta \delta Y_H + Y_A \theta (1-\alpha_2)(1-\beta)) z_{4,q} \overline{XS} \cdot DO^*_t \\
& + (\alpha_2 \beta \delta Y_H + Y_A \theta (1-\alpha_2)(1-\beta)) z_{5,q} \overline{DOX} \cdot S^*_t \\
& + ((\alpha_2 \beta \delta Y_H + Y_A \theta (1-\alpha_2)(1-\beta)) z_{6,q} \overline{SDO} - \widetilde{D_q} \cdot \eta_X) X^*_t \\
& - k_d \cdot X_t
\end{aligned}
\tag{B.11}
$$

$$
\begin{aligned}
DO_t - DO_{t-1} = \sum_{q \in Q} \Big(& \widetilde{D_q} \cdot DO^*_{in,t} \\
& - ((\alpha_2 \beta \delta (1-Y_H) + (4.57 - Y_A) \theta (1-\alpha_2)(1-\beta)) z_{7,q} \overline{XS} - \widetilde{D_q} \cdot (1-\gamma_{DO})) DO^*_t \\
& - (\alpha_2 \beta \delta (1-Y_H) + (4.57 - Y_A) \theta (1-\alpha_2)(1-\beta)) z_{8,q} \overline{XDO} \cdot S^*_t \\
& - (\alpha_2 \beta \delta (1-Y_H) + (4.57 - Y_A) \theta (1-\alpha_2)(1-\beta)) z_{9,q} \overline{SDO} \cdot X^*_t \\
& - \frac{OU_{20} \cdot h}{V \cdot DO^{sat}} \overline{Air} \cdot DO_t \\
& + \frac{OU_{20} \cdot h}{V} \cdot Air_t
\end{aligned}
\tag{B.12}
$$

Appendix C Inflow categories

Appendix D Derivation of $w_1 = 1$ and $w_2 = 0$

The premise for including the airflow rate as an input to the reduced order model is that the resulting oxygen transfer rate (OTR) matches the OTR calculated for the full ASM1 using the oxygen transfer coefficient kLa:

$$
\frac{(OU_{20} \cdot h_{aer})}{(V \cdot DO^{sat})} \cdot Air \cdot (DO^{sat} - DO) = kLa \cdot (DO^{sat} - DO) \tag{D.1}
$$

The left-hand side of this equation can be simplified according to Equations :

$$
\frac{(OU_{20} \cdot h_{aer})}{(V \cdot DO^{sat})} \cdot Air \cdot (DO^{sat} - DO) = \frac{(OU_{20} \cdot h_{aer})}{V} \cdot Air - \frac{(OU_{20} \cdot h_{aer})}{(V \cdot DO^{sat})} \cdot Air \cdot DO \tag{D.2}
$$

According to Smets et al. (2006), the product of the DO concentration and the Airflow can be approximated as:

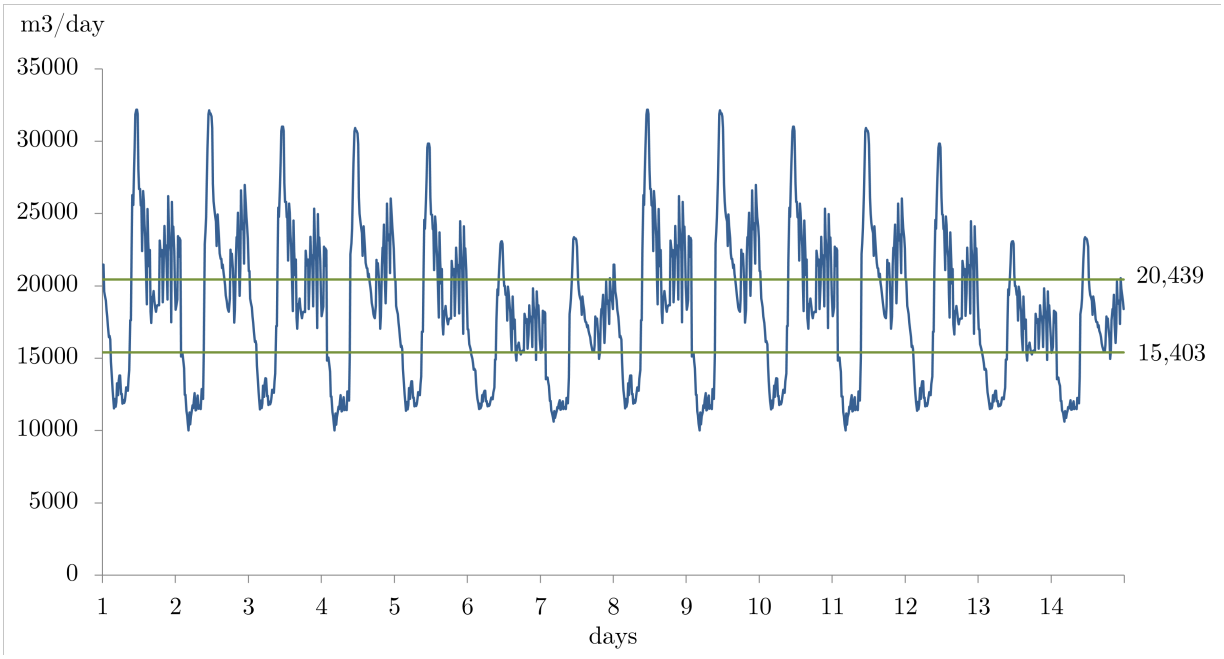

Figure C.1: Limits of influent flow categories in the linear reduced-order model

$$DO \cdot Air \approx (w_1 \overline{Air} DO + w_2 Air \overline{DO}) \tag{D.3}$$

Which then yields for the second term on the right-hand side of Equation D.2:

$$\frac{(OU_{20} \cdot h_{aer})}{(V \cdot DO^{sat})} \cdot Air \cdot DO \approx \frac{(OU_{20} \cdot h_{aer})}{(V \cdot DO^{sat})} \cdot (w_1 \overline{Air} DO + w_2 Air \overline{DO}) \tag{D.4}$$

Replacing this on the left-hand side of Equation D.1 and writing the terms explicitly yields:

$$\frac{(OU_{20} \cdot h_{aer})}{(V \cdot DO^{sat})} \cdot Air \cdot DO^{sat} - \frac{(OU_{20} \cdot h_{aer})}{(V \cdot DO^{sat})} \cdot (w_1 \overline{Air} DO + w_2 Air \overline{DO}) = kLa \cdot DO^{sat} - kLa \cdot DO \tag{D.5}$$

Isolating the terms that are a function of DO yields:

$$-\frac{(OU_{20} \cdot h_{aer})}{(V \cdot DO^{sat})} \cdot (w_1 \overline{Air} DO + w_2 Air \overline{DO}) = -kLa \cdot DO \tag{D.6}$$

Following this, w_1 is

$$w_1 = \frac{kLa \cdot V \cdot DO^{sat}}{\overline{Air} \cdot OU_{20} \cdot h_{aer}} \tag{D.7}$$

According to Rieger et al. (2006), kLa can be defined as:

$$\delta \cdot kLa = \delta \frac{(OU_{20} \cdot h_{aer})}{(DO^{sat} \cdot V)} \cdot Air \tag{D.8}$$

Substituting kLa in Equation D.7 yields

$$w_1 = \frac{Air}{\overline{Air}} \tag{D.9}$$

With the model assumption of a constant airflow $\overline{Air}$, this finally yields $w_1 = 1$.